SOLUTION MINING RESEARCH INSTITUTE
679 Plank Road
Clifton Park, NY 12065, USA

Telephone: +1 518-579-6587
www.solutionmining.org

Technical Conference Paper

1965 – 2025

High-Resolution Acoustic Imaging for Large Diameter Inspections: Multi-Cavern Case Studies

Zachary Evans, DarkVision, North Vancouver, Canada

Lydia Richley, DarkVision, North Vancouver, Canada

SMRI Fall 2025 Technical Conference
29-30 September 2025
Wichita, Kansas, United States

Solution Mining Research Institute Fall 2025 Technical Conference

Wichita, Kansas, United States 29-30 September 2025

HIGH-RESOLUTION ACOUSTIC IMAGING FOR LARGE DIAMETER INSPECTIONS: MULTI-CAVERN CASE STUDIES

Zachary Evans and Lydia Richley

DarkVision Technologies, North Vancouver, Canada

Abstract

High-resolution acoustic imaging for large-diameter casing inspections represents a new standard in cavern inspections, offering a more precise and intuitive approach for operators to proactively maintain their wells. By providing direct, sub-millimetric measurements and complete circumferential coverage, this technology overcomes the limitations of traditional inspections that struggle to address cavern-specific challenges.

The benefits of high-resolution acoustic imaging for cavern operators are significant. Chief among these is the capability to inspect both the internal and external surfaces of large-diameter pipes with medical-grade precision, enabling a comprehensive understanding of corrosion, wall thinning, and defect growth over successive inspections. Additionally, this enables operators to perform more advanced and accurate burst pressure calculations such as Effective Area or RSTRENG, which are not possible when utilizing low-resolution devices. Moreover, the high-resolution acoustics visualizations and integrity analysis of downhole components, such as casing shoes, and completed remedial work like expandable liners and casing patches improves operators' understanding of their assets and ability to plan for the future.

This paper highlights the value and capabilities of high-resolution acoustic imaging for cavern operators over legacy devices and presents multiple operator case studies of large-diameter casing inspections that explore issues such as ovality, connections, expandable liners, and casing patches.

Introduction

The value of high-resolution acoustic imaging, as discussed in this paper, is best understood when viewed against the current challenges facing cavern operators:

- ***Large Casing Diameter and Wall Thickness***

  With current technologies, logging large-diameter casing (16" and above) is possible, but offers low resolution and is often limited to measurements on the casing's internal diameter (ID) only.

- ***Minimal Focus on Cavern-specific Concerns***

  Key concerns include wall thinning, defect progression, corrosion, burst pressure, and the integrity of downhole components. Operators increasingly seek to identify the root causes of wall thinning to accurately assess burst pressure, which requires obtaining measurements from both the internal diameter (ID) and external diameter (OD) of the casing.

- ***Limitations of Existing Inspection Tools***

  Minimal innovation over recent decades leaves operators reliant on a narrow set of logging technologies. These tools have seen little advancement, highlighting significant opportunities for improvement. These technologies are discussed in detail in the following section.

Limitations of Current Technologies

Technologies commonly employed for well-integrity inspections face a variety of challenges:

- Multi-Finger Calipers (MFC) offer low-resolution datasets and require contact with the casing wall which can introduce errors due to dynamic effects and decentralization and risks of sensor liftoff. This technology operates with a ‘finger gap' or incomplete circumferential coverage.
- Magnetic Flux Leakage (MFL) tools infer wall loss by measuring the loss of magnetic flux and correlating this lost flux signal to a modeled calibration response. These devices struggle with complex corrosion patterns, gradual wall loss, and subtle defects like splits and cracks, thereby limiting their effectiveness.
- Pulse Eddy Current (PEC) devices pulse a magnetic field in the casing to analyze the rate of eddy current decay when the signal is cut off. An average thickness reading is then calculated using calibrated values based on ideal casing specifications. Due to this averaging and non-representative calibration information, PEC tools cannot accurately assess thickness in areas with complex corrosion and varying casing specifications.
- Single-element ultrasonics offer limited spatial resolution and azimuthal coverage, making them less effective in providing repeatable defect detection. The legacy device’s low coverage and low-resolution dataset is likely to miss critical defects and misrepresent the casing’s condition and risk profile, as supported by conclusions from Tao et al. (2024). Furthermore, these tools require multiple runs to swap heads for assessing wells with varying casing diameters which is not the case with the high-resolution acoustic imaging tool.

High-Resolution Acoustic Imaging Technology Overview

High-resolution acoustic imaging, introduced by Robinson et al. (2020), surpasses traditional cased-hole inspection tools by delivering high-fidelity, 3D direct measurements of inner diameter (ID) and outer diameter (OD) wall loss defects. This technology operates in a liquid-agnostic and fully circumferential manner, providing superior resolution and performance. The tool combines a solid-state piezoelectric sensor and innovative imaging techniques to achieve an imaging resolution of 0.25 mm (0.01 in). With up to 512 individual transducers arranged around the tool’s circumference, the solid-state array allows for electronic beam focusing and steering, enabling the assessment of multiple casing sizes in a single run. Proprietary software and advanced imaging modes control the wavefronts generated by the transducers, compensating for decentralization and tool eccentricity. An image of this high-resolution acoustic imaging tool is shown in Figure 1.

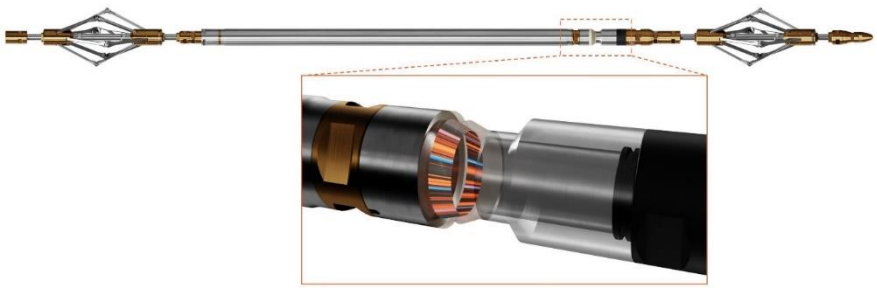

Figure 1: High-resolution acoustic radial imaging tool captures sub-millimetric (0.25 mm) inner casing surface measurements for assessing wall loss defects, breaches, deformation, threaded connection makeup, and completions hardware.

The technology's combination of comprehensive and intuitive visualizations with direct measurement at 0.25 mm resolution has greatly improved the ability to detect, size, and characterize critical defects, as well as identifying malfunctioning subsurface equipment. This is done by providing accurate and detailed inspection of the casing ID, OD, thickness, corrosion, pitting, breaches, thread damage, over-torqued connections, parted casing, perforated/engineered punches, deformation, and ovality.

Acoustic Imaging Methods

Depending on the application, the high-resolution acoustic technology uses a combination of direct and diffuse imaging modes to capture submillimeter measurements of both the inner and outer casing surfaces.

Diffuse Imaging to Evaluate ID Surface Texture

Robinson et al. (2020) demonstrated how capturing diffuse acoustic reflections from a casing ID enables this technology to produce high-fidelity, textured renderings of the surface, facilitating the detection of corrosion, erosion, scale buildup, and other complex features or components. Following contact with a defect on the casing surface, the incoming angled acoustic wavefront refracts off the textured casing surface and produces multiple echoes and a scattering of diffuse waves. Analyzing the diffuse acoustic signals returned to the angled imaging probe enables the creation of high-fidelity images and direct measurements of the casing's surface at 0.25mm resolution regardless of casing surface geometry. Figure 2 illustrates the principle of diffuse reflection imaging.

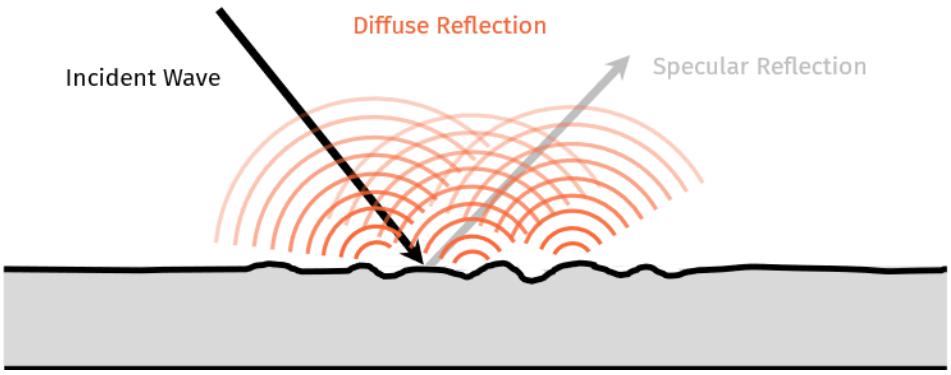

Figure 2: Simulation depicting diffuse reflection imaging and how this unlocks improved surface textural assessment and ID measurements.

This approach creates significant advantages in detecting and measuring small holes, complex corrosion, pinholes, breaches, or other interacting defects. Figure 3 shows an unwrapped acoustic intensity view or acoustic amplitude visualization showing a 3.0 mm through-casing pinhole found inside of a region with broader general corrosion. The complexity of this defect would make it challenging for legacy integrity assessment tools to detect, size, or depict the true nature of the breach.

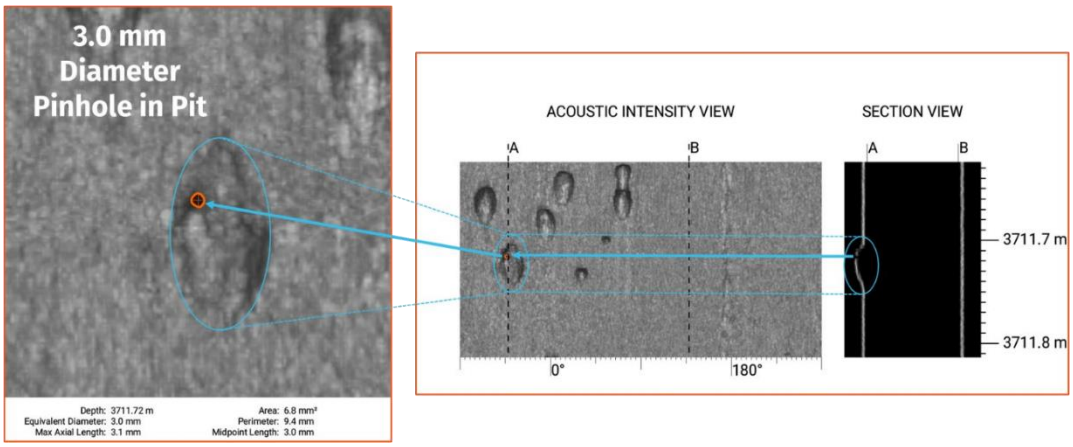

Figure 3: 3.0 mm Pinhole in Pit assessed from a downhole log using diffuse reflections from the acoustic imaging technology.

Direct Reflection Imaging to Evaluate Casing Thickness

Direct reflection enables this technology to “see through the steel” and directly measure casing thickness, including assessing corrosion and external wall loss defects. Figure 4 presents sequential simulation images to explain the process by which casing thickness is measured. First, a high-frequency wave is emitted from the transducer (frame 1) and travels through the fluid medium towards the casing (frame 2). Energy is reflected immediately after hitting the inner wall of the casing, and some is absorbed by the steel, where it continues to propagate to the outer casing wall (frame 3). The acoustic energy continues to oscillate inside the steel, and with each contact of the inner or outer surface, it creates a wavefront that propagates back to the sensor (frame 4).

The first signal represents the ID wall profile, followed by any indication of wall loss, and the complete signal of the OD of the casing. By recording the acoustic signal's travel time between the ID, defect, and OD at the probe, and factoring in the known speed of sound in the fluid and casing, a precise map of the casing's ID and OD surfaces can be generated, allowing for accurate determination of the remaining wall thickness at the defect locations. Laboratory validation of these measurements across a variety of different thicknesses and defect types is discussed by Simpson et al. (2022).

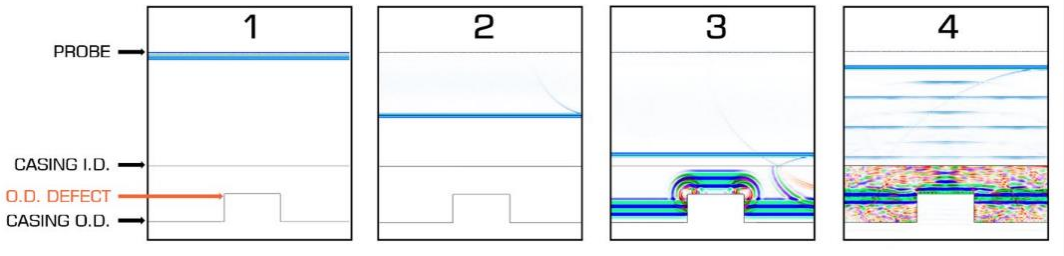

Figure 4: Simulation depicting high-frequency signal transmission and reflections used to evaluate casing thickness.

Using High-Resolution Acoustic Imaging for Advanced Burst Pressure Calculations

The improvement in resolution presented by high-resolution acoustic imaging has also facilitated the use of more accurate burst pressure calculations. Figure 5 illustrates the various burst pressure methodologies employed by the American Society of Mechanical Engineers (ASME), arranged from the most pessimistic and least accurate to the least pessimistic and most accurate (ASME, 2012). Legacy inspection devices lack the resolution and run-over-run repeatability required to use more advanced methodologies, such as Effective Area and RSTRENG.

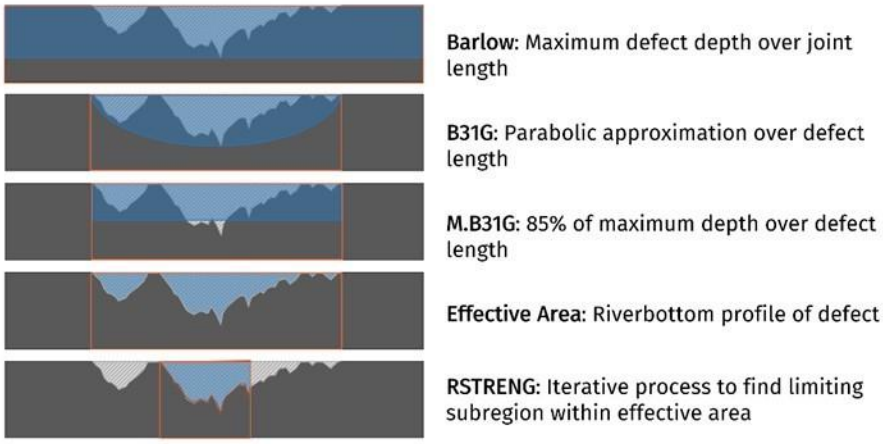

Figure 5: Burst pressure methodologies from ASME in order from least accurate on top, Barlow, to most accurate at the bottom, RSTRENG.

The high-resolution output of acoustic imaging has facilitated a stepwise improvement in analysis methodology and reduced pessimism. Simpson et. al (2022) demonstrated how the detailed river bottom profiles of defects produced by high-resolution acoustic imaging can be combined with advanced burst pressure calculation methods to provide a more accurate burst pressure, especially in complex and interacting defects. The ability to accurately assess defects in terms of surface radial measurement, wall loss compared to nominal casing, and axial and circumferential characterization, allows for the reliable calculation of multiple burst pressure methodologies.

Figure 6 shows an example of the advanced burst pressure analysis prepared using this technology to assess a defect. A zoomed-in image of the limiting defect and its river bottom profile is shown in the plot on the right as a blue shape and the calculated burst pressure values on the left in the Limiting Defect Summary. The ability to accurately size this defect's axial length, utilized by the Effective Area calculation, gives a maximum burst pressure much higher than that determined by Barlow – where only the maximum defect depth is considered.

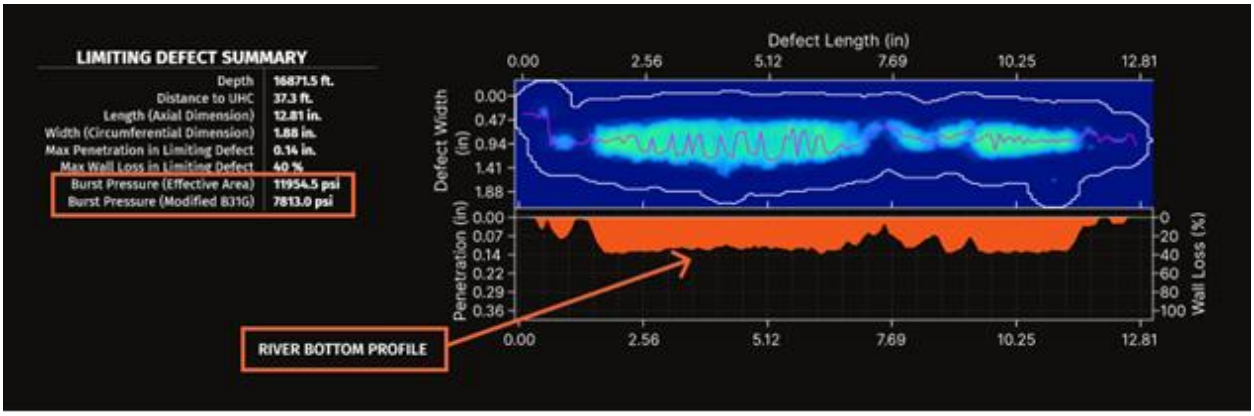

Figure 6: Limiting defect burst pressure assessment of the limiting defect in a casing joint with 40% wall loss.

Advanced Visualizations Enabled by High-Resolution Acoustic Imaging

Various visualization types are used to intuitively present the data captured.

Figure 7 shows three examples that illustrate the versatility of high-resolution acoustic imaging. From left to right, the first shows an acoustic intensity map featuring a small axial split – a feature that would have been missed by other tools. This intensity map is exclusive to the diffuse imaging response and is valuable for visualizing breaches and other unique and subtle surface texture features that create a visible response compared to the surrounding healthy casing. The second example shows how 3D point clouds of data are used to generate a precise 3D rendering of a damaged liner hanger. Lastly, a 2D log shows the thickness measurements of a gas storage well that indicates the successful placement of an expanded liner.

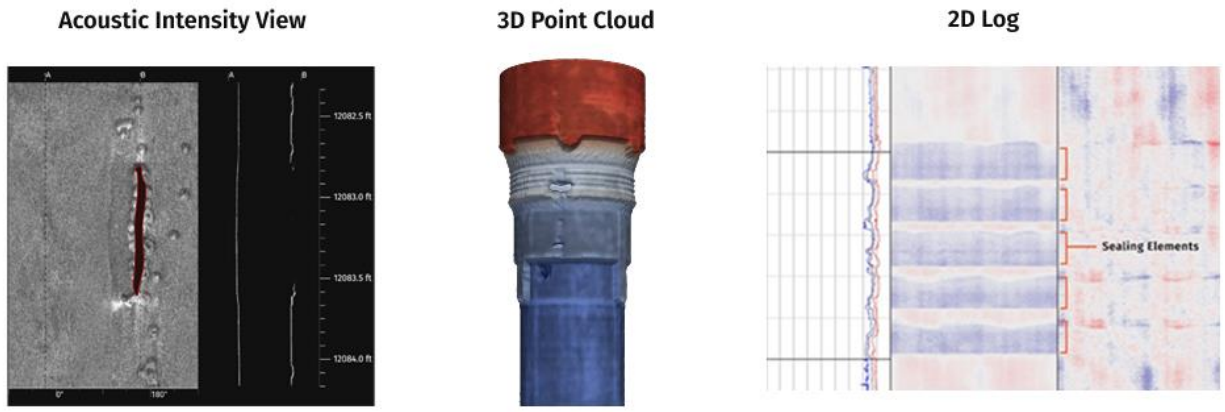

Figure 7: Examples of different visualization methods for acoustic results.

Cavern Operator Deployment Case Studies

With this detailed understanding of the high-resolution acoustic technology and its visualization capabilities, this section showcases three unique case studies to highlight its capabilities in cavern wells with casing sizes up to 24-inches. Before presenting the case studies, the following section describes the common form of data presentation, the 2D log.

Log Presentation

In presenting the findings of the case studies explored in this publication, a 2D log format is used to visualize the various forms of data captured using the ultra-high-resolution acoustic imaging platform. For reference in reviewing the following examples, an annotated summary of the data tracks presented in this log format is provided below in Figure 8.

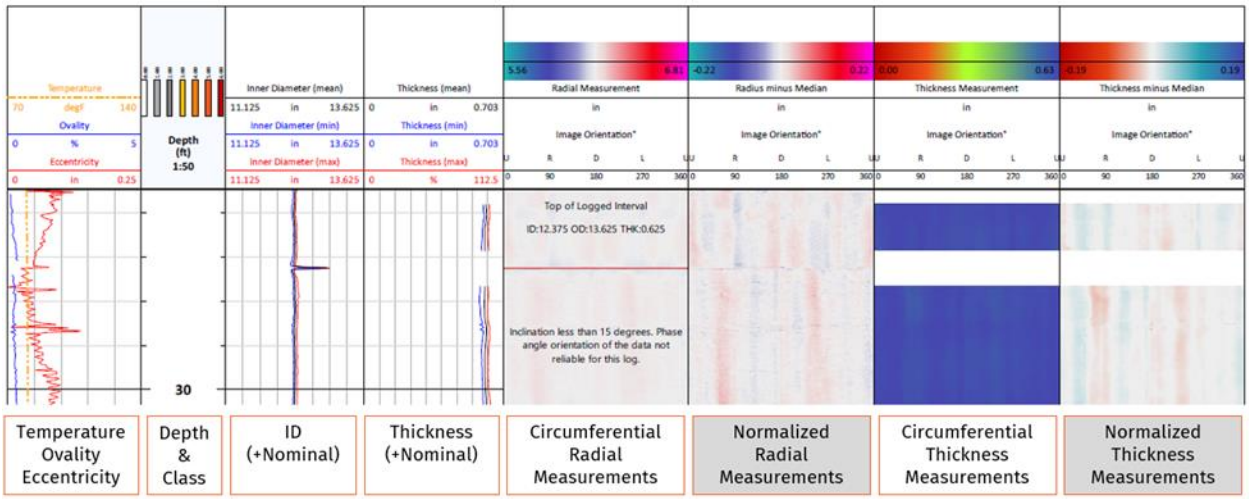

Figure 8: Log data track descriptions.

Case Study #1: Verifying an Expandable Liner in 16” Casing.

Having lab-validated the technologies’ ability to assess casing thickness (Simpson et al 2022) and advancing the imaging and analysis process for large diameter, thick wall casings, efforts then shifted to

the solicitation of an appropriate field trial candidate. From these efforts, a Gulf Coast natural gas storage cavern well was selected for this initial field test.

The subject well was completed with 4,100’ of 16” production casing and based on available well documentation contained both 0.75” & 0.812” wall X-52 pipe with welded connections. The primary objective was to fulfill standard regulatory requirements for routine casing inspections, and secondarily to evaluate the placement and condition of an expandable liner installed during the preceding workover over a milled casing window. While no other areas of concern were highlighted ahead of inspection, the operator expected some degree of ovalization or deformation near the cavern ceiling, which is common in active salt cavern storage and solution mining wells.

During deployment, care was taken to monitor on-surface data in real time to confirm robust data quality. Ultimately, data was successfully acquired at logging speeds between 20-30 ft/min, with a standard brine serving as the in-situ liquid, an ideal conduit for acoustic coupling.

The first finding quickly identified was that the provided documentation and operator assumptions regarding the weight and configuration of the installed casings were inaccurate. While it was expected that the up-hole section of the string would be the lighter pipe listed as 0.75” wall, the acoustic technology’s direct physical measurements confirmed the upper 2,408’ of the 16” casing to be 0.812” in thickness with a 14.376” ID. This confirmation of nominal pipe characteristics ensures that any metal loss or ovalities found in this region would be evaluated correctly against accurate nominal pipe values, rather than over or under-calling metal loss based on a flawed thickness assumption. The next segment of pipe, extending from 2,408’ to 4,100’, similarly did not match records and was measured to have a 0.85” wall with a 14.3” ID.

Owing to the radial probe's diffuse imaging, which is unaffected by changes in pipe geometry or component complexity, an evaluation of the connections in this well was also possible. One connection at 4,047.6' was identified as anomalous and exhibited a larger than expected internal diameter, extending consistently and uniformly across the full circumference of the pipe. This internal groove appears to be the result of an imperfect weld in which material has moved away from the interior of the pipe during the joining process (Figure 9 and Figure 10). Figure 11 shows a nominal connection, highlighting the stark difference between the two. While mechanical in nature, this feature will be monitored for future growth.

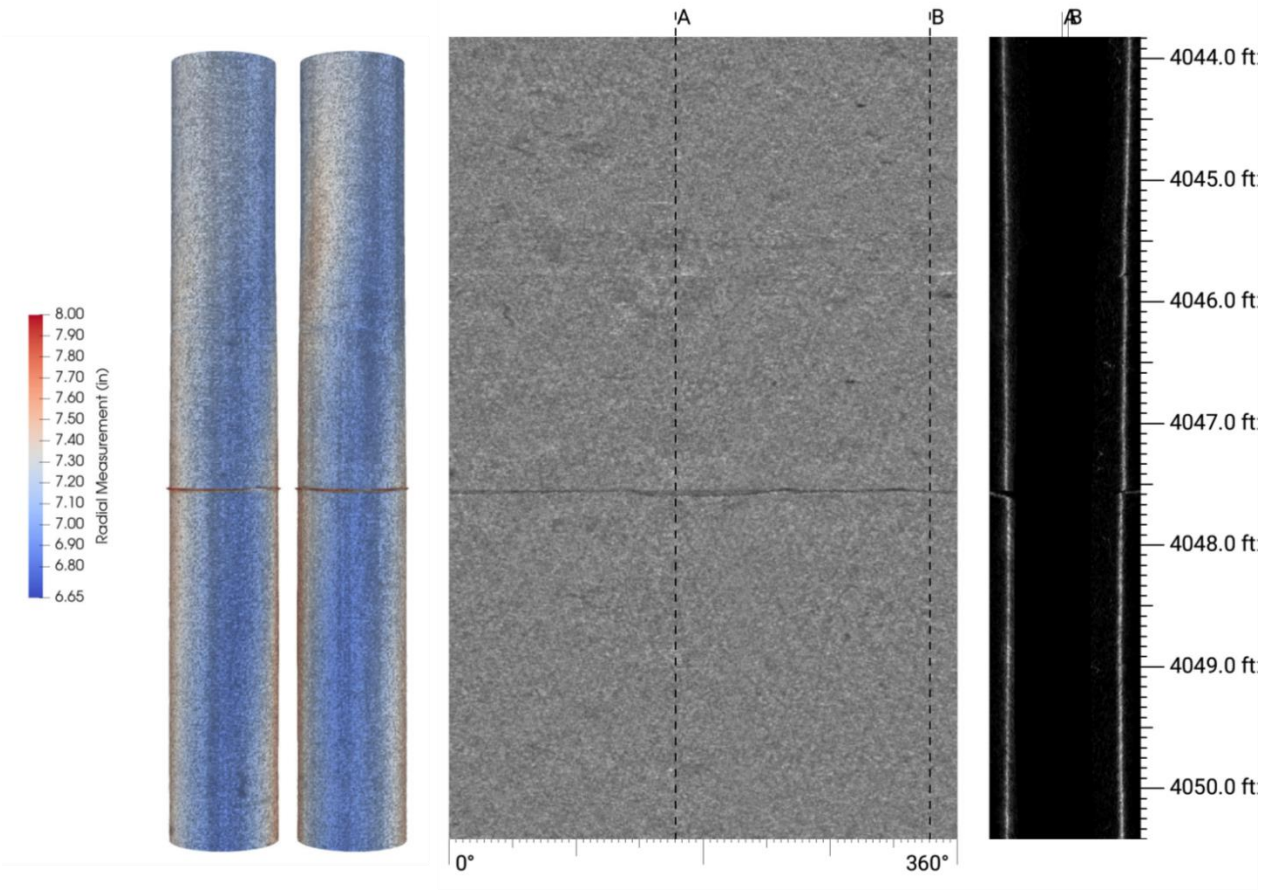

Figure 9: 3D render (left), Acoustic Intensity Image (middle), and axial section (right) of internal pipe surface showing abnormal connection.

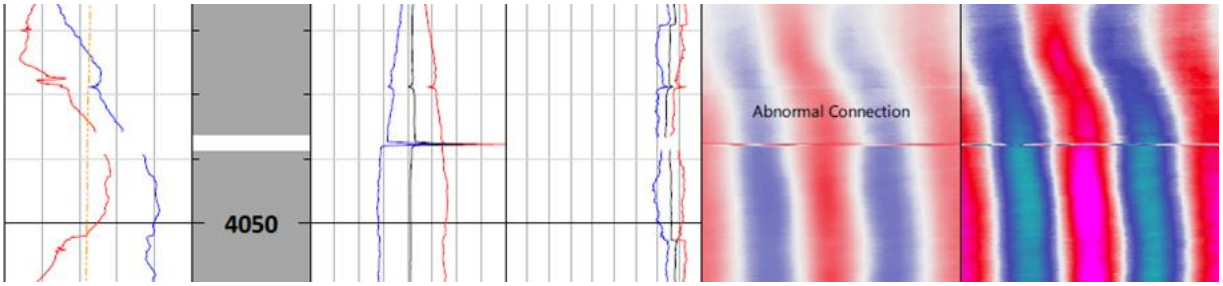

Figure 10: Abnormal connection at 4,047.6'.

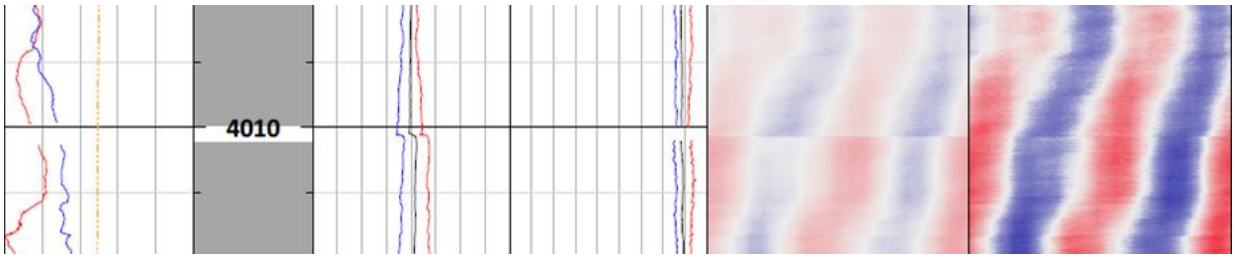

Figure 11: Nominal connection immediately up-hole of abnormal connection at 4,010.2'.

Evaluating the casing string for metal loss features, no significant corrosion or mechanical damage was discovered. Metal loss features ranged from 7-19%, with a maximum penetration of 19% observed at 1,508.1' in an isolated external pit. Given standard pipe manufacturing tolerances of 12.5%, most defects fall at or below a reasonable expectation of initial pipe condition out of the mill. Additionally, with such large pipe, variations in manufacturing patterns are expected, allowing for a practical application of reason when evaluating minimal penetration percentages as seen in this case. High-resolution acoustic measurements were able to accurately identify minor wall loss down to a minimum value of 9% in this thickest section of pipe, with that percentage translating to an identified penetration of just .08" (Figure 12).

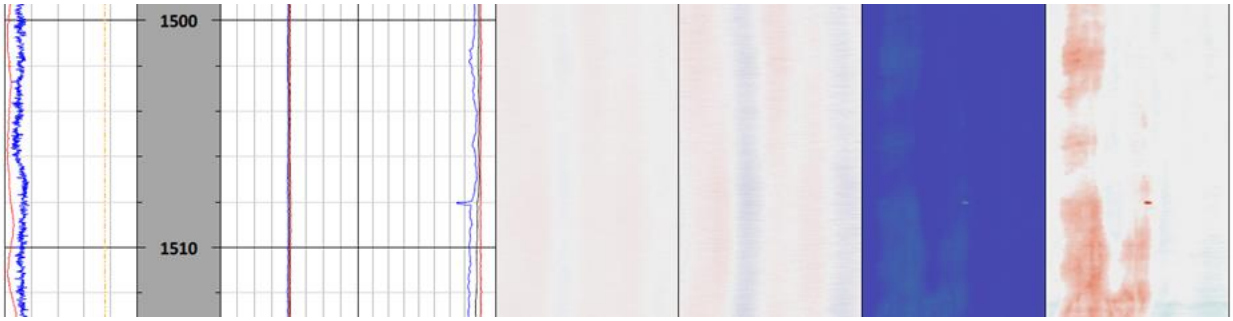

Figure 12: Maximum metal loss feature of 19% at 1,508.1'.

As expected, the casing string did exhibit a considerable amount of ovalization in the regions nearing the top of salt, with a maximum ovality of 8.31% measured at 4,050' (Figure 14). Quantifying ovality in this region is valuable for future regulatory inspections as it should be accounted for if corrosion or other metal loss defects are found within the ovalized zone.

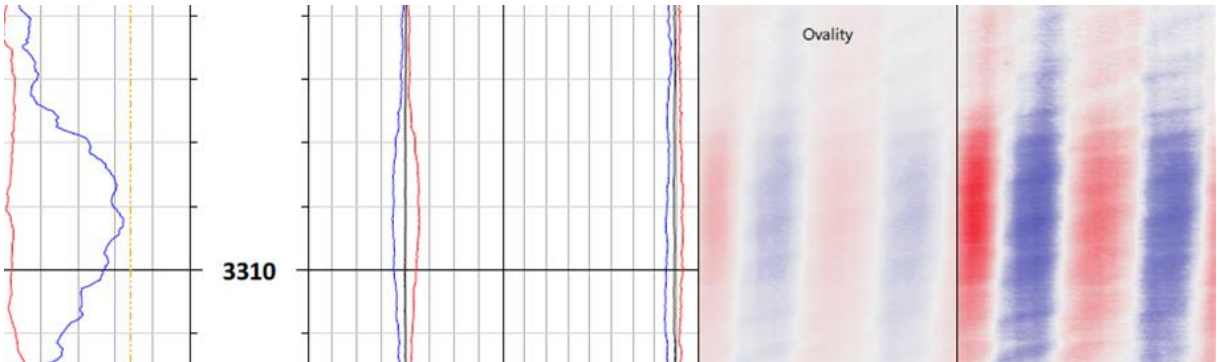

Figure 13: Example of localized ovality measuring 3.23% showing uniform deformation at 3,308'.

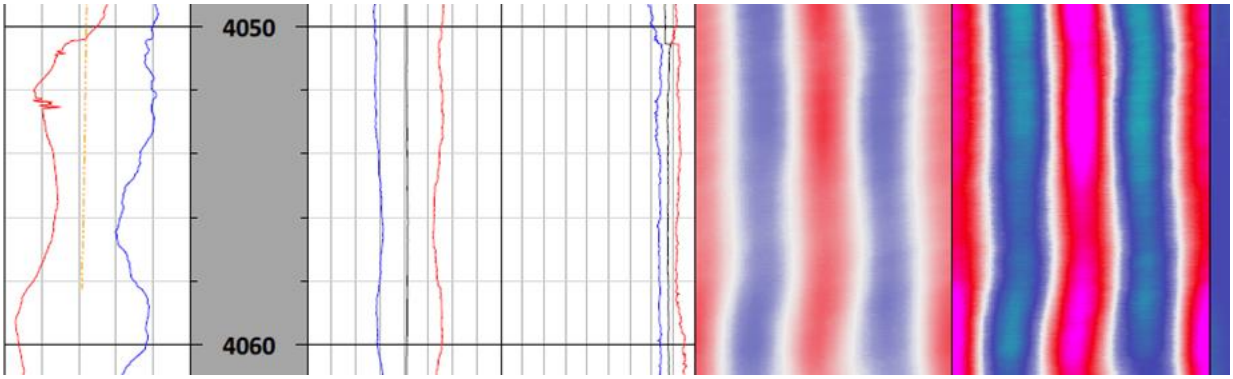

Figure 14: Significant region of general ovalization measuring 8.31% immediately above casing shoe at 4,050'.

An additional unexpected feature was discovered at 3,990', where a restriction was detected in what appeared to be an area of buildup or debris as indicated by a significant reduction in diameter through this region (Figure 15). The minimum ID measurement of 12.86" was exhibited at the point of maximum buildup compared to a nominal expected inner diameter of 14.3". While this feature was not included in any of the available pre-job well information, discussions with the operator revealed that a temporary packer had been set at this depth and topped off with sand and resin, with this debris then being residual material that remained after drill-out operations.

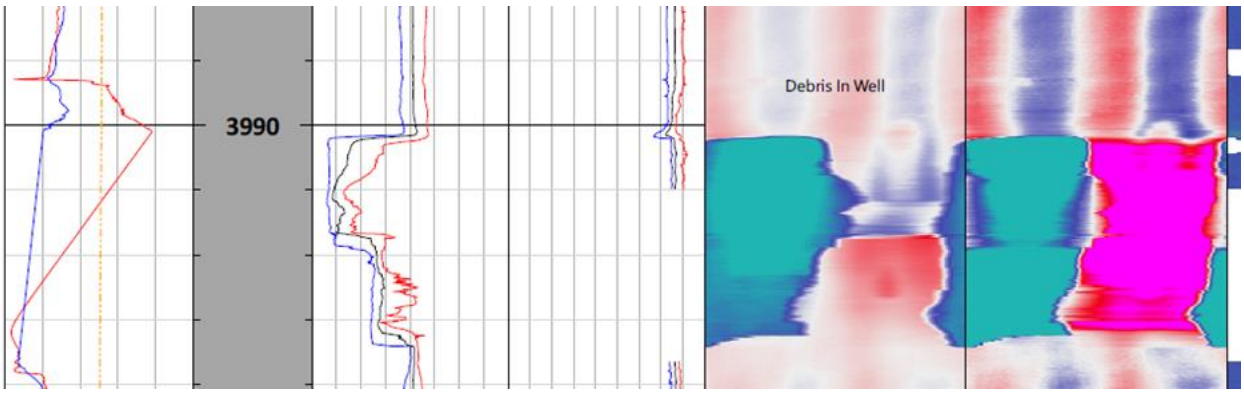

Figure 15: Log representation of Debris.

A secondary objective was to inspect the placement and condition of an expandable liner previously run to cover a milled window. Using high-resolution acoustic measurements, not only was the liner located in terms of axial placement and scanned internally for any damage, but the technology was also able to confirm the expanded diameter and wall thickness of the liner against manufacturer specification.

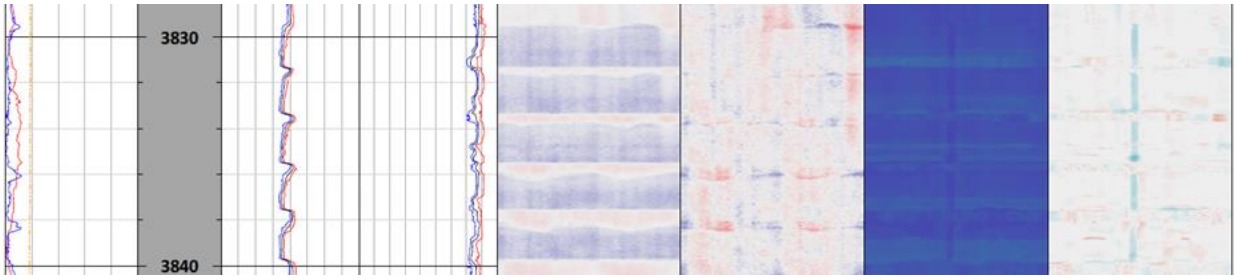

Figure 16: Upper sealing elements of expandable liner at 3,830'.

The visible top of the liner was encountered at 3,829’ where the upper elastomer sealing elements of the liner could be observed, as shown in Figure 16. When expanded, these seals create a slight relief in the internal pipe surface, as the surrounding metal material expands further than the metal with the sealing material directly behind it. This creates a very distinct pattern in the radial ID measurements which can easily be used to confirm placement over the zone of interest. This same pattern can be observed at the bottom of the liner at 3,942’ where the distinct variations in internal diameter as also detected (Figure 17).

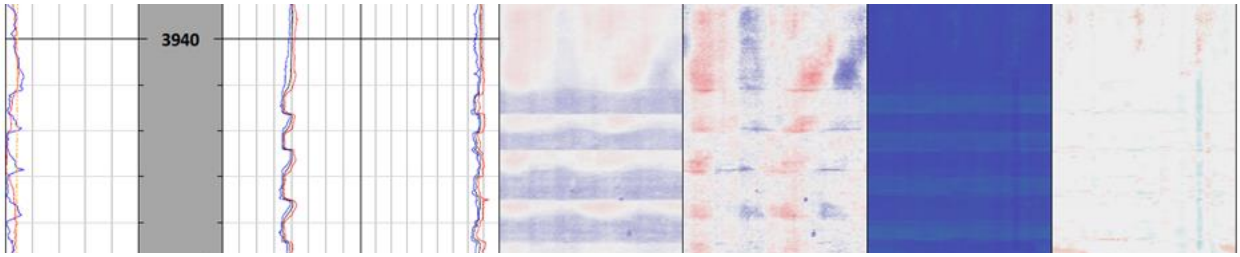

Figure 17: Lower sealing elements of expandable liner at 3,942'.

Based on the manufacturing specification sheet provided by the operator for this specific liner product, after expansion, the liner should display an internal diameter of 13.490” and a wall thickness of 0.371”. While some regions of the liner did show ovalization which caused varied ID measurements, non-ovalized segments of the liner were measured as having the exact ID and wall thickness characteristics as expected based on manufacturing guidance.

In summary, the use of high-resolution acoustic measurements to measure both the internal characteristics and wall thickness of a 16” diameter casing string with a thickness of up to 0.85” proved to be a resounding success, with accurate measurements meeting strict internal data quality standards acquired through the entirety of the well. This log helped establish a real-world baseline for deploying high-resolution acoustics in this application, which was crucial in the advancement of using this technology to service the well integrity and inspection needs of the salt cavern market. In addition, these results allowed the operator to confirm the successful deployment of an expandable liner, identify a previously unknown residual debris restriction, and gave them the necessary integrity information regarding connection health, corrosion, and deformation

that will allow them to meet regulatory requirements as well as safely and efficiently operate this facility in the future.

Case Study #2: 20” Diameter Casing Inspection

A second well from the same Gulf Coast salt cavern storage facility was inspected with the objective of expanding proven capabilities up to 20” diameter casings with a nominal wall thickness of 1.0”.

This well contained a mixed string, roughly 3,984’ in total, of both 20” diameter, 203 ppf welded line pipe with a wall thickness of 1.0” as well as a lower section of 20”, 250 ppf welded line pipe with an expected thickness of 1.25”, both of an unknown grade.

As in the previous example, while the primary focus of this logging run was to fulfill routine regulatory requirements for casing inspections, the operator indicated multiple regions of priority based on previous diagnostics, including minor drilling wear or rotational damage at 1,320’ and 2,000’. In addition, the operator wanted to investigate minor corrosion which was concentrated up-hole, as well as various regions of ovalization, and a specific anomaly at 2,530’ that was the suspected result of a previous string shot. As with the previous trial, tool running speed and brine quality were monitored in real-time at surface to ensure the successful acquisition of data.

In analyzing the results of this run, a review of the data confirmed the expected internal diameter and wall thickness of the up-hole pipe section, which extended from surface to 3,417’, as 18” and 1.0” respectively. Results also showed expected welded connections, all of which appeared intact and without damage or deformation. In some joints, the presence of the manufacturing weld seam could be observed along with very minor manufacturing patterns typical of new, modern tubulars (Figure 18).

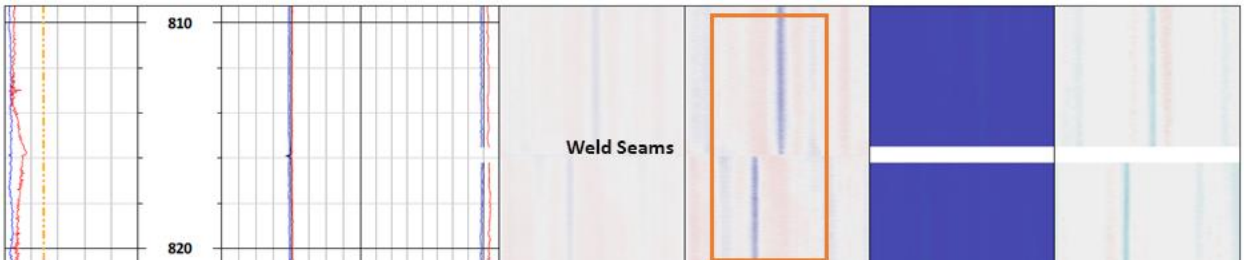

Figure 18: Example of visible weld seams in two adjacent joints at 816'.

depth of 3,417’, where the pipe transitioned to an inner diameter of 17.5” and a wall thickness of 1.25”.

In investigating the presence of corrosion, mechanical damage, or other metal loss features, almost no defects were found throughout the entirety of the well, revealing a casing string with minimal well integrity concerns. In total, only 3 unique joints showed metal loss above the API manufacturing tolerance for new pipe of 12.5%, with a maximum penetration of 19%, or 0.19”, at a depth of 1,394.8’ in the region of expected corrosion. In these 3 joints, all of which are adjacent and run from 1,295’ to 1,415.7’, all metal loss features are associated with a uniform vertical defect on the interior of the pipe (Figure 19). While this feature appears to be distinct from the manufacturing weld seam, it could be a function of mechanical damage due to the running of tools or drill wear, as the feature is uniform in its axial orientation and extends across connections without a change in profile. These results confirm the presence of minor metal loss seen near 1,320’ identified by previous logs but reveals the true nature of the defect being mechanical in nature and not organic corrosion. The direct measurements confirmed that features previously reported at 2,000’ were inaccurate.

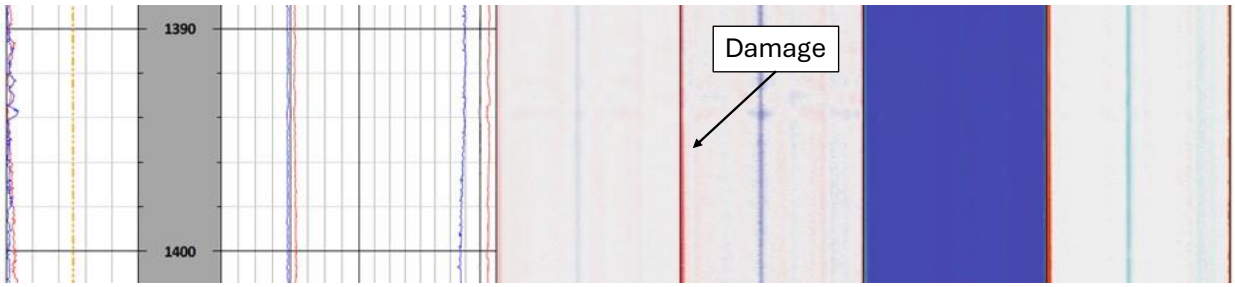

Figure 19: Maximum wall loss feature of 19% at 1,394.8' associated with internal damage.

Investigating the suspected damage caused by string shot at 2,530', a generalized region of internal metal loss was observed at 2,526', as shown in Figure 20. Measurements in this region show a larger than expected minimum internal diameter of 17.96", potentially indicating metal loss of 0.02". There is, however, no associated change in wall thickness, indicating that this region of pipe has been displaced but has not seen actual metal loss due to damage or indentation. This finding is of critical importance to the operator in evaluating future well integrity concerns, as even though the minor change in profile will ultimately affect the casing's burst pressure profile, the pipe still retains its full wall thickness.

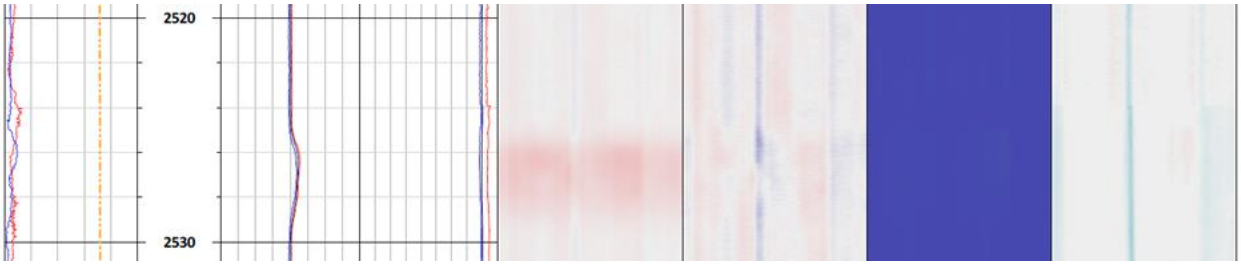

Figure 20: Region of internal damage likely caused by string shot at 2,526'.

In general, this casing string did not exhibit any actionable metal loss features, with only four defects above manufacturing tolerances and a total metal loss range of 3-19%. It is important to note the level of precision available via high-resolution acoustic measurements, as the identification of metal loss extends to 3% of nominal wall thickness, which translates to just .03" of penetration.

Ovalization was present in the expected regions, beginning at 2,620’ and appearing sporadically through the remainder of the well. All instances were below an actionable threshold with a maximum ovality of 2.58% being measured at a depth of 3,278’ (Figure 21).

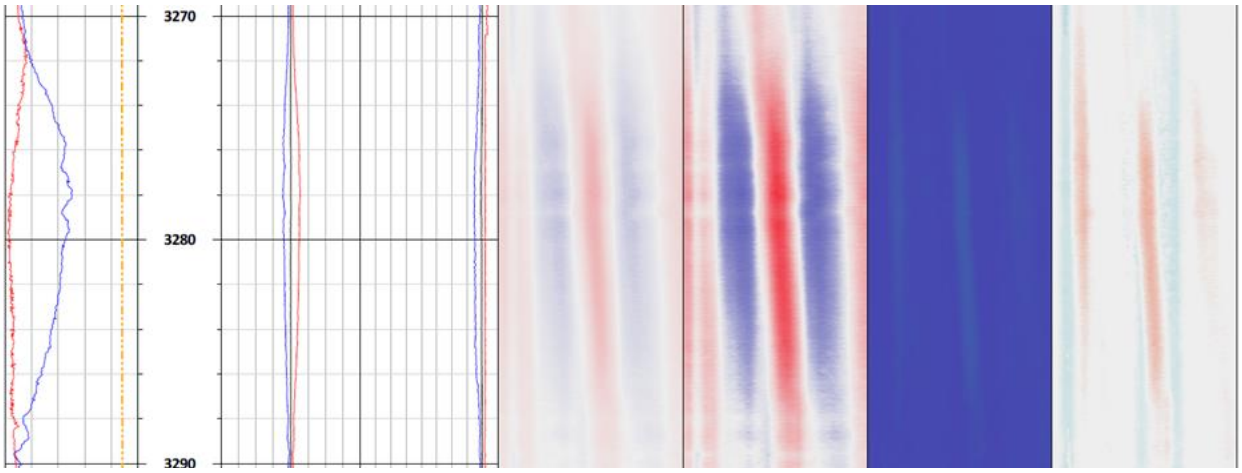

Figure 21: Maximum ovality of 2.58% at 3,278'.

Direct, high-resolution acoustic measurements also revealed two unexpected features. First, a restriction was observed, shown in Figure 22. This feature, roughly 1’ in length, presents a region of uniform build up with a minimum diameter of 15.72”, restricting wellbore access from the nominal ID of 18” and the joint specific average ID measurement of 17.91”. The operator noted that this was potentially the remnants of a previously installed downhole component.

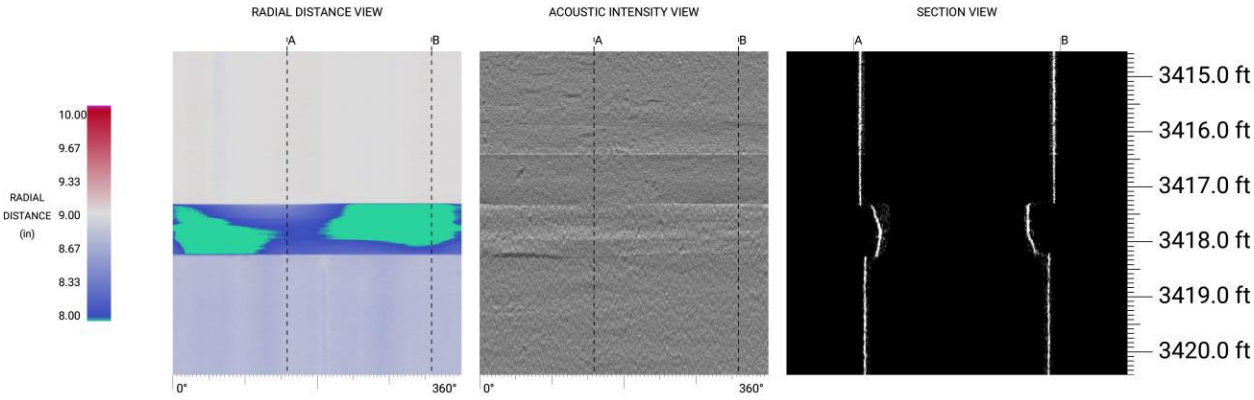

Figure 22: Debris restriction at 3,420' associated with previous plug setting.

Finally, a minor region of metal loss was observed near the bottom of the scanned interval at 3,924’ (Figure 23). Radial measurements in this area are like those observed in the region of suspected string shot

damage. However, there is an associated decrease in wall thickness across this zone. This indentation near the shoe is likely the result of a retrievable plug or similar sealing component. The contrast between this metal loss feature and the metal moved feature highlighted previously at 2,526' shows the value of accurate thickness measurements to truly understand and characterize downhole features in instances where inner diameter caliper measurements may prove insufficient.

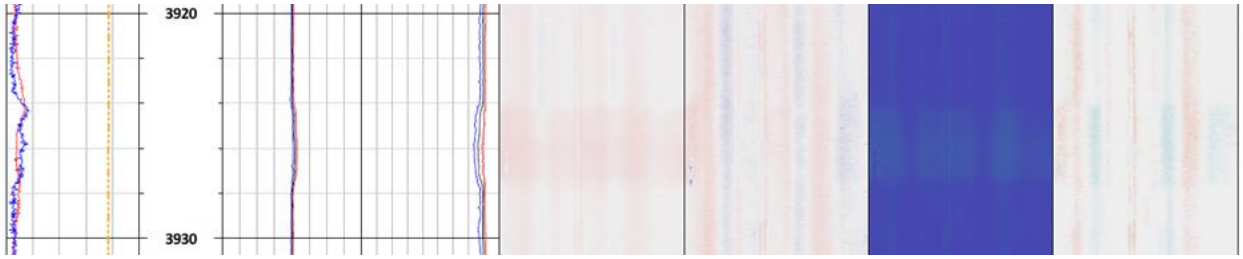

Figure 23: Minor casing anomaly at 3,924' potentially associated with previous plug setting.

In summary, high-resolution acoustic measurements were again validated in large pipe applications, confirming the technology's capabilities in pipe up to 20" in outer diameter and 1.25" in wall thickness. This dataset confirmed and accurately quantified previous areas of expected metal loss and ovalization, refuted areas where legacy technologies had inaccurately raised concerns, and identified previously unknown restrictions and metal loss potentially caused by previous workover operations. Most importantly, this data provided full coverage of the mixed casing string, providing assessments of both internal and external metal loss, and confirmed the lack of well integrity concerns and general positive health of the well tubulars.

Case Study #3: Baseline Logging of a 24" Cavern Well

Having confirmed the viability and capability of high-resolution acoustic measurements in the thickest casing to be encountered in practical downhole operations, a final field trial was completed with the goal of proving successful deployment of the technology in the largest diameter of casing in common use. The practical upper limits of casing diameter and wall thickness commonly encountered in the cavern space is 24" OD, 1" wall casing, with many operators standardizing around this design for new cavern wells in the future.

The well selected for this case study came from an additional Gulf Coast cavern operator, though in this case, it is not a natural gas storage well like the previous two case studies and is instead a newly converted liquid storage cavern well. The selected well is completed with a 24" 245.87 ppf API 5L-X-52/56 production string with a nominal wall thickness of 1.0" and welded connections.

To appropriately centralize the acoustic tools, specific centralizers were manufactured as a purpose-built solution. Four sets of Large Casing Centralizers (LCCs) were machined with 2.5" wheels and maximum arm extension of 21.15". To maximize centralization, both the radial and thickness tools were centralized above and below the probe to best ensure consistent axial orientation. However, as the centralizer arms are spring-loaded, the assemblies can collapse as necessary to easily pass through any restrictions or changes in diameter, overcoming concerns regarding rigidity of the bottom hole assembly. Furthermore,

due to the physics of ultrasonic technology not requiring physical contact with the pipe being investigated, only the roller wheels of the centralizers contact the inner surface of the pipe, further increasing the tool's ability to travel at a consistent speed and adapt to a changing inner casing profile, shown in Figure 24.

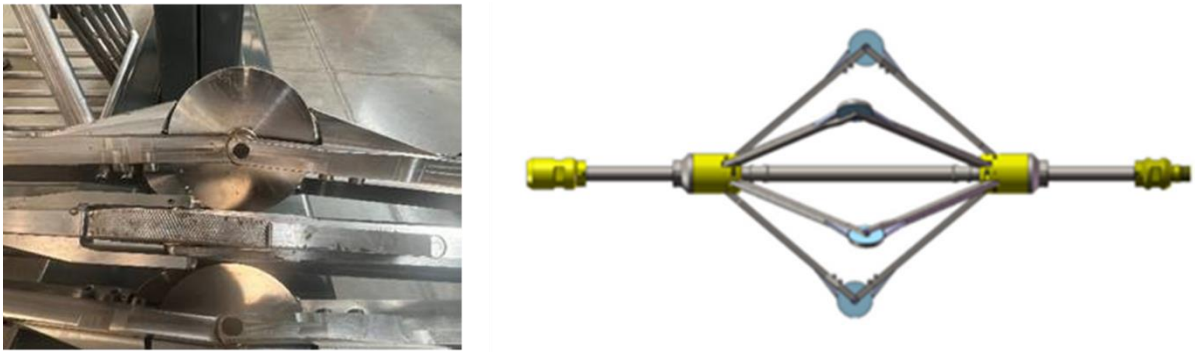

Figure 24: Left, a photograph of the manufactured LLCs and, right, a tool string diagram representation.

Initial analysis of the dataset confirmed the expected weight and size of pipe as 22” ID with a nominal wall thickness of 1.0”. While this is essentially guaranteed given the new nature of the well and its installed tubulars, confirmation of pipe condition remains a crucial preliminary diagnostic, as instances of discrepancies against expected pipe condition have been observed even in newly drilled wells with recently installed tubulars.

A unique pattern of debris was found at 24’, where a roughly 3’ circumferential band of internal buildup was observed, shown in Figure 25. However, this region of debris does appear to be friable as radial measurements show clear linear low spots in the debris pattern. These are likely caused by logging tool centralizers passing through the debris while running into the well. In discussion with the operator, other cased-hole logs had shown an unexpected response in this region as well.

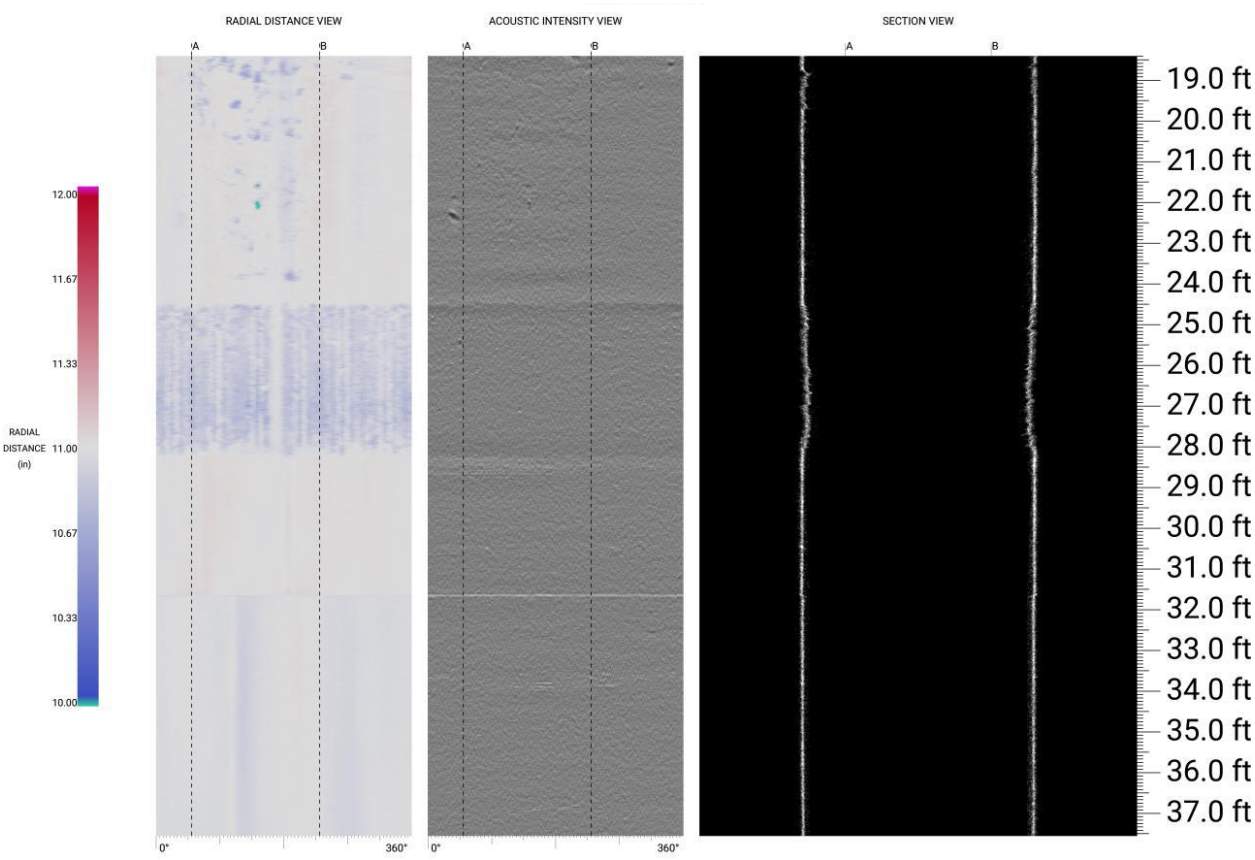

Figure 25: Multiple visual representations of buildup observed at 24'.

Further investigating the data set for the presence of metal loss, only 2 joints were found with defects above the standard 12.5% API tolerance for new pipe manufacturing, and in both instances the defects measured 0.13” of reduced internal radius compared to nominal, for a percentage deviation of just 13%, and were aligned with the joint’s weld seam which is clearly visible in many joints (Figure 26). In total, metal loss features, or imperfections from milling, were found in the range of 3-13%, indicating healthy pipe and establishing a clear baseline with sub-millimetric precision that can be accurately used in future inspections. Even at an inner diameter of 22” and with a pipe wall thickness of 1.0”, high-resolution acoustic measurements are capable of reporting single-digit changes in pipe thickness, in this case ranging as low as 0.03” in variation for a percentage penetration of just 3%.

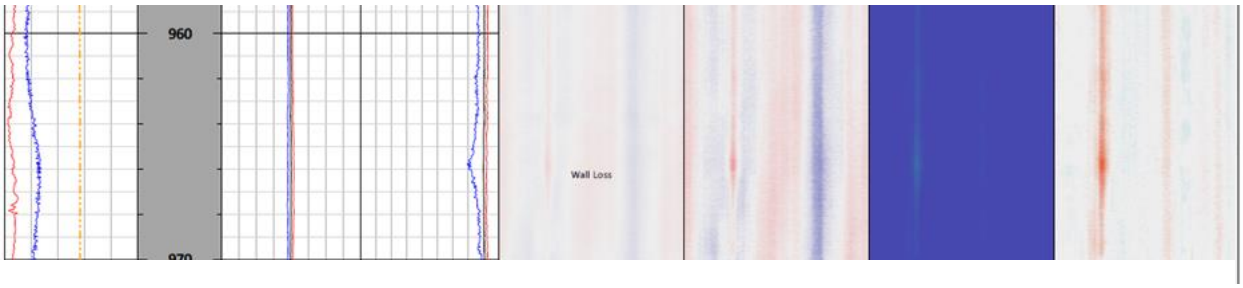

Figure 26: Joint exhibiting 13% metal loss from nominal at 965.8'.

Evaluation of the welded connections in the casing string yielded no areas of concern, as all connections were observed to be intact and without damage. Observation of the connections also confirms the presence of the weld seam in most joints (Figure 27).

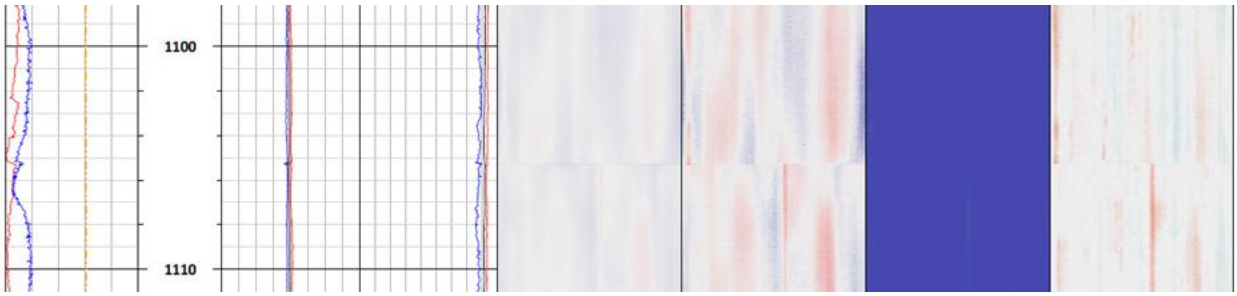

Figure 27: Example of a healthy connection at 1,105' also showing a weld seam observable in the lower joint but not upper pipe.

Traditional technologies are negatively impacted by the large metal mass of the wellhead as are legacy tools with pads that cannot safely exit the bottom of the casing string. In contrast, high-resolution ultrasonic technology can inspect the pipe, but also the wellhead, casing shoe, and in the case of salt caverns, the chimney or neck of the salt cavern.

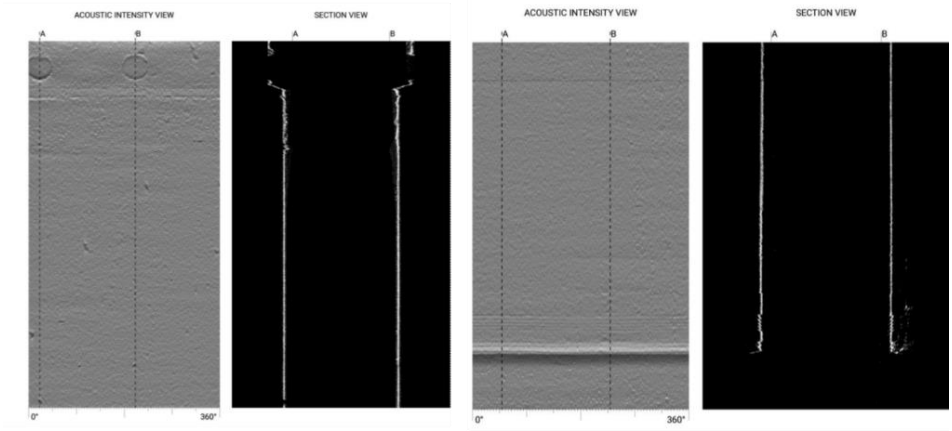

Figure 28: Left, Acoustic intensity and axial section of lower ports and, right, acoustic intensity and axial section view of cavern neck.

In this case study, the fluid top reached the top of the casing into the hanger and lower elements of the assembly, providing a clear image of the lowermost ports (Figure 28). This capability allows for maximum coverage of near surface casing condition up to and including the hanger, which avoids the limitations of legacy technologies unable to detect or quantify near surface corrosion due to physical limitations associated with the wellhead. Similarly, the ability to drop the radial probe of the tool string through the casing shoe and into the cavern neck allows for the same kind of fully comprehensive evaluation of the string, examining not only the condition of the shoe but also the cavern neck, measuring and imaging any potential washouts.

Analysis also revealed an undocumented component in the string, as seen in Figure 29, likely to be a float collar based on acoustic profile and location in the well as discussed with the operator. This highlights the ability of direct measurements to detect all features within a casing string regardless of pre-job documentation, allowing for a complete well schematic and wellbore diagram to be created after inspection for future risk assessment purposes.

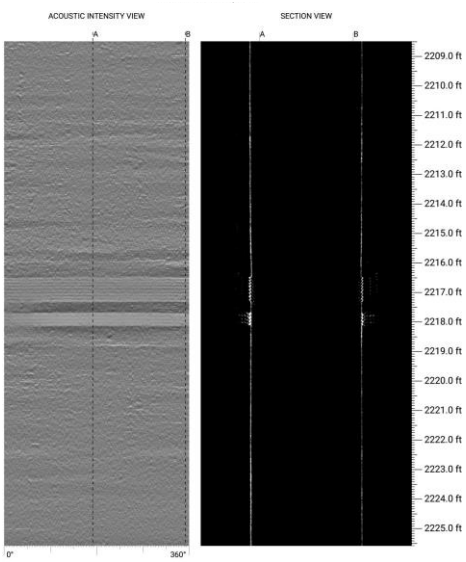

Figure 29: Potential float collar detected at 2,216'.

Additionally, a variety of slip marks were found when evaluating the external surface of the pipe (Figure 30). These marks, created immediately above and below the connections while handling and running casing into the wellbore, do not indicate regions of metal loss or indentation, but rather simply external regions of the pipe that have been polished by the placement of casing handling tools. While this was not necessarily a primary diagnostic goal of the logging run, it is notable that this level of precision - identifying minor textural differences on the outer diameter of 24" casing through a 1.0" thick pipe wall - is possible using high-resolution acoustics.

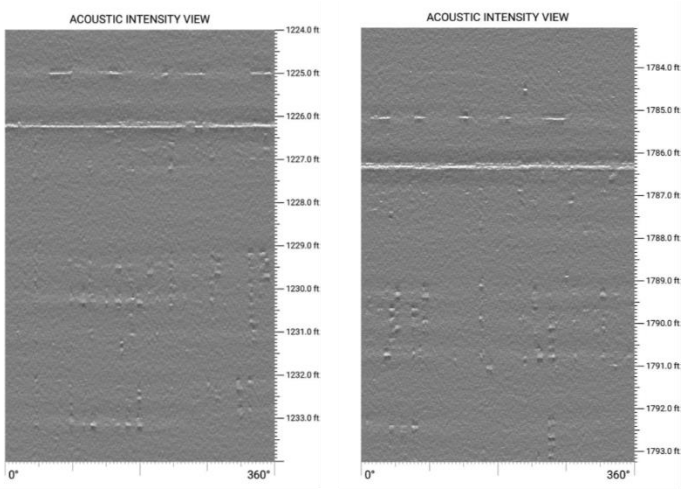

Figure 30: Example of external casing slip marks at 1,226' and 1,786'

In conclusion, this casing inspection validated the capabilities of high-resolution acoustic imaging technology in evaluating the internal and external condition of casing at the upper limits of industry standard tubulars in both diameter and thickness of pipe. It also provided precise, holistic baseline inspections of a new liquid cavern well, confirming the expected healthy condition of all casing joints and connections as well as a qualitative assessment of the wellhead, casing shoe, cavern neck, and all downhole components.

Conclusions

High-resolution acoustic imaging provides direct, sub-millimetric measurements and complete circumferential coverage of both the ID and OD of cavern casings. The cavern market historically has not had access to high resolution imaging to inspect their large diameter and thick wall completions. This technology overcomes the limitations of legacy devices and unlocks insights specific to cavern market concerns such as wall thinning, deformation, corrosion, and burst pressure in thick, large diameter casing.

The validation and field trials outlined in this paper demonstrate the successful deployment of this technology to inspect casing diameters up to 24” and casing thickness of up to 1.25”, demonstrating the following:

- Single run logging and assessment of a variety of casing weights and thicknesses.
- Validation of casing specification records and ability to provide corrections when inconsistencies are found.
- Ability to inspect and characterize complex components such as casing shoes, float collars, expandable liners and wellheads.
- Accurate differentiation between metal loss vs. metal moved, provided by the combination of ovality/deformation characterization and wall thickness measurements, as highlighted in Case Study 2.
- Utilization of more accurate burst pressure calculations, such as Effective Area. This allows operators to safely maximize the life of the well and minimize expensive and unnecessary remediations.
- Validation of connection type and integrity. High-resolution acoustics are uniquely advantaged in their ability to detect and analyze pipe weld seams and welded connections for integrity.
- Streamlined root cause analysis and confident remediation via intuitive visuals and precise measurements of both defects and their contextual region.
- Confirmation of the presence (of lack of) previously reported features, as seen in the Case Study 2.
- Accurate baseline logging of new pipe, enabling regulatory compliance and detailed run over run monitoring.

Acknowledgements

The authors of this manuscript would like to acknowledge and thank the industry partners who made this research and field testing possible. Without this generous collaboration from industry leaders in the salt cavern storage space, the previously referenced case studies would not have been possible.

Specifically, the authors would like to thank Chase Ringer of Boardwalk Pipeline Partners and Thomas Garcia of ONEOK for graciously facilitating the field trials by providing practical large diameter casing inspection scenarios in active salt cavern wells. Similarly, the authors would like to thank Kyle Kelley and Brandon Schulte of STRATA for their logistical oversight and project management of the associated logging jobs allowing for successful field deployment and execution of these trials.

References

American Society of Mechanical Engineers (ASME). Manual for Determining the Remaining Strength of Corroded Pipelines: Supplement to ASME B31 Code for Pressure Piping. ASME B31G-2012. ASME, New York, NY (2012).

Robinson, Stephen , Littleford, Thomas , Luu, Tim , Wardynski, Kacper , Evans, Andrew , Horton, Blake , and Michael Oman. "Acoustic Imaging of Perforation Erosion in Hydraulically Fractured Wells for Optimizing Cluster Efficiency." Paper presented at the SPE Hydraulic Fracturing Technology Conference and Exhibition, The Woodlands, Texas, USA, February 2020. doi: https://doi.org/10.2118/199718-MS

Tao, G, Doan, Q, Islam, A, Abdulhameed, D, Scoging, A, & Cardiff, S. "Evaluation of High-Resolution Downhole Tubular Inspection Tools by Full-Scale Field Testing." Proceedings of the 2024 15th International Pipeline Conference. Volume 2B: Pipeline and Facilities Integrity. Calgary, Alberta, Canada. September 23–27, 2024. V02BT03A003. ASME. https://doi.org/10.1115/IPC2024-133711

Simpson, Greer, Littleford, Tom, and Anthony Battistel. "High-Resolution Acoustic Imaging for Submillimetric Casing Thickness Quantification and Advanced Effective-Area-Based Burst Pressure Analyses." Paper presented at the SPE Annual Technical Conference and Exhibition, Houston, Texas, USA, October 2022. doi: https://doi.org/10.2118/210010-MS

Alatigue, M. F., Egbe, P. I, Aljedawi, R., and T. Pehlke. "Revolutionizing Complex Casing Integrity Analysis in the Middle East Using High-Resolution Acoustic Imaging." Paper presented at the ADIPEC, Abu Dhabi, UAE, November 2024. doi: https://doi.org/10.2118/222949-MS

Creaform3d. 2024. 2024 Technical Documents, https://www.creaform3d.com/blog/technical-documents/ (accessed 17 July 2025).